Polymer nanocomposites enhance S-nitrosoglutathione intestinal absorption and promote the formation of releasable nitric oxide stores in rat aorta

Wen Wu, Caroline Perrin-Sarrado, Hui Ming, Isabelle Lartaud, Philippe Maincent, Xian-Ming Hu, Anne Sapin-Minet, Caroline Gaucher

Dear Author,

Please, note that changes made to the HTML content will be added to the article before publication, but are not reflected in this PDF.

Note also that this file should not be used for submitting corrections.

ELSEVIER
Nanomedicine: Nanotechnology, Biology, and Medicine
xx (2016) xxx–xxx
nanomedicine
Nanotechnology, Biology, and Medicine
nanomedjournal.com

Polymer nanocomposites enhance *S*-nitrosoglutathione intestinal absorption and promote the formation of releasable nitric oxide stores in rat aorta

Wen Wu, PharmD, PhD[a], Caroline Perrin-Sarrado, PharmD, PhD[a], Hui Ming, PharmD[a], Isabelle Lartaud, PharmD, PhD[a], Philippe Maincent, PharmD, PhD[a], Xian-Ming Hu, PhD[b], Anne Sapin-Minet, PhD[a], Caroline Gaucher, PhD[a,*]

[a]*CITHEFOR EA3452 "Drug targets, formulation and preclinical assessment", Faculté de Pharmacie, Université de Lorraine, Nancy, France*
[b]*State Key Laboratory of Virology, Ministry of Education Key Laboratory of Combinatorial Biosynthesis and Drug Discovery, Wuhan University School of Pharmaceutical Sciences, Wuhan, China*

Received 16 October 2015; accepted 5 May 2016

Abstract

Alginate/chitosan nanocomposite particles (GSNO-acNCPs), *i.e.* *S*-nitrosoglutathione (GSNO) loaded polymeric nanoparticles incorporated into an alginate and chitosan matrix, were developed to increase the effective GSNO loading capacity, a nitric oxide (NO) donor, and to sustain its release from the intestine following oral administration. Compared with free GSNO and GSNO loaded nanoparticles, GSNO-acNCPs promoted 2.7-fold GSNO permeation through a model of intestinal barrier (Caco-2 cells). After oral administration to Wistar rats, GSNO-acNCPs promoted NO storage into the aorta during at least 17 h, as highlighted by (i) a long-lasting hyporeactivity to phenylephrine (decrease in maximum vasoconstrictive effect of aortic rings) and (ii) *N*-acetylcysteine (a thiol which can displace NO from tissues)-induced vasodilation of aortic rings preconstricted with phenylephrine. In conclusion, GSNO-acNCPs enhance GSNO intestinal absorption and promote the formation of releasable NO stores into the rat aorta. GSNO-acNCPs are promising carriers for chronic oral application devoted to the treatment of cardiovascular diseases.

Key words: NO-donor; Polymer nanocomposites; Oral delivery; Isolated aorta vasoreactivity

In the cardiovascular system, deficiency of endogenous nitric oxide (NO) is the consequence of either insufficient synthesis (endothelium dysfunction)[1,2] or excessive NO degradation[3,4] (increased oxidative or nitrosative stresses, decreased antioxidant enzyme activity). NO depletion is one of the key factors in the initiation and progress of many diseases, such as atherosclerosis,[5] pulmonary hypertension,[6] thrombosis,[7] ischemia[8] and cardiac arrhythmia.[9] To maintain an appropriate level of NO and treat NO deficiency, several NO-related therapeutics have been developed such as nitrosamines, organic nitrates, metal–NO complexes, *N*-diazeniumdiolates. However, all act at very short term and lead to tolerance phenomena. *S*-nitrosothiols (RSNOs) present the advantage of a longer half-life, with no tolerance nor oxidative stress induction. Under physiological conditions, *S*-nitrosoglutathione (GSNO), a major endogenous RSNO, is one of the main storage forms of NO in tissues.[10] GSNO has been investigated for its powerful antiplatelet activity,[11,12] arterio/venous selective vasodilator effects,[13,14] antimicrobial[15] and antithrombotic effects.[16]

Despite such therapeutic potencies, GSNO pharmaceutical forms are still lacking. This may be related to the fast and often unpredictable rate of decomposition of GSNO. *In vitro*, because of pH-, light- and temperature-dependent sensitivities, GSNO is susceptible to many degradation processes

Funding and conflicts of interest: This work was supported by the 'Université de Lorraine and Région Lorraine'. W. Wu and H. Ming acknowledge Chinese Scholarships Council for their doctoral fellowships. X.-M. Hu was a guest professor at the Université de Lorraine, CITHEFOR EA 3452, for three months between 2014 and 2015.

The funders had no role in study design, data collection and analysis, decision to publish, or preparation of the manuscript.

*Corresponding author.
E-mail address: caroline.gaucher@univ-lorraine.f (C. Gaucher).

http://dx.doi.org/10.1016/j.nano.2016.05.006
1549-9634/

including *S*-NO bond homolysis, metal ion-catalyzed decomposition, and hydrolysis. *In vivo*, it is subjected to enzymes-induced decomposition such as GSNO reductase[17] and carbonyl reductase 1.[18] For this reason, the bioavailability of GSNO when administrated orally is limited. Two main strategies were described to overcome such limitations, through either inhibiting GSNO reductases activity[19] or improving the stability of GSNO. In respect to the latter, many researchers focused on the protection of GSNO – during storage and in biological media – through the combination with delivery systems to promote pharmaceutical and medical applications. For instance, Seabra and co-workers dispersed GSNO into polyethylene glycol (PEG)[20] or solid poly(vinyl alcohol)/poly(vinyl pyrrolidone) film[21] to achieve the controlled release of NO adapted to topical application. de Mel and co-workers passively incorporated GSNO into a polyhedral oligomeric silsesquioxane poly(carbonate-urea)urethane (POSS-PCU) composite to produce a NO realizing implant for cardiovascular diseases treatment.[22] Encapsulation followed by *S*-nitrosation of glutathione (GSH, the GSNO precursor) into mucoadhesive polymeric nanoparticles produced GSNO loaded nanoparticles, which slowed down GSNO decomposition at physiological temperature.[23,24] Similarly, Shah et al described another way to prolong the release of NO by conjugating GSH on chitosan backbone and *S*-nitrosating the GSH thiol group.[25] In our previous work, polymeric nanoparticles based on poly(methyl)methacrylate were developed to load GSNO through direct encapsulation (GSNO-NP), which protect GSNO and preserve its availability during interaction with smooth muscle cells.[26] However, the release profile we obtained was not long enough for chronic *in vivo* therapeutic applications. In our following work,[27] we developed polymer nanocomposite particles (NCP), which refer to nanoparticles of nanometric size embedded in a polymer matrix forming a composite particle of micrometric size, as defined by Bhattacharya and coworkers.[28] Microparticles were composed in our case of an alginate or a chitosan matrix including our previously described GSNO-NP.[26] These GSNO-NPs embedded into chitosan or alginate nanocomposites increased the encapsulation efficiency of GSNO compared to GSNO-NPs (from 54% to 69% or 76%, respectively) and sustained the *in vitro* release of GSNO until 24 h.[27]

From these promising results, in the present study, our aims were to further improve GSNO oral bioavailability, to control its delivery at the absorption site and to prolong the residence time into the gastrointestinal tract, by combining both alginate plus chitosan in the matrix. Alginate and chitosan were chosen as mucoadhesive polymers increasing the residence time on the intestine mucus layer.[29-32] As alginate has the capacity to penetrate the mucus layer,[30] this will bring the drug closer to the intestinal cells, while chitosan exerts the property to open cells tight junction.[31,32] Therefore, their combination will lead to increase drug permeability through the intestine. To broke new ground in the field of nanocomposite particles and merge mucopenetration and mucoadhesion properties in one system, we therefore developed GSNO-loaded alginate/chitosan nanocomposite particles (GSNO-acNCPs) formed through the incorporation of GSNO-NPs into a mix of alginate/chitosan matrix. The efficient encapsulation capacity and the sustained release profile of GSNO encouraged us to further investigate GSNO permeability through an intestinal cell barrier model (Caco-2). Finally, for the first time, we administrated GSNO-acNCPs to Wistar rats by gavage in order to evaluate their vascular effects, more particularly their capacity to increase the NO-storage inside the vascular wall.

Methods

Materials

All reagents were of analytical grade and all solutions prepared with ultrapure deionized water (>18.2 mΩ.cm at 25 °C). Sodium nitrite was purchased from Merck (Germany). Acrylates/ammonium methacrylate copolymer (Eudragit® RL PO) was a generous gift from Evonik industries (Germany). Alginate sodium, chitosan (4-6 kDa), polyoxyethylene-polyoxypropylene block copolymer (Pluronic® F-68), mucin from porcine stomach, HBSS with Ca^{2+} and Mg^{2+} and all other reagents were obtained from Sigma-Aldrich (France). All experiments and assays involving GSNO were conducted under conditions of subdued light and at +4 °C in order to minimize light- and temperature-induced GSNO degradation.

Methods

GSNO synthesis

GSNO was synthesized according to a previously described method.[33] Briefly, reduced GSH was incubated with an equivalent of sodium nitrite under acidic condition (0.626 M HCl); after precipitation, the solid form of GSNO was obtained. The purity of GSNO was assessed by HPLC and UV spectrophotometry using the specific molar absorbance of the *S*-NO bond at 334 nm (ε = 922 $M^{-1}cm^{-1}$).

Preparation of GSNO-loaded alginate/chitosan nanocomposite particles

GSNO-loaded alginate/chitosan nanocomposite particles (GSNO-acNCPs) were constituted by inner cores and external polymer matrix. The inner cores were GSNO-loaded nanoparticles (GSNO-NP) prepared by a double emulsion (water–oil–water) and solvent evaporation method as described in previous work.[26] Briefly, an aqueous solution containing GSNO in 0.1% (w/w) Pluronic® F-68 was emulsified by sonication with an organic phase containing Eudragit® RL PO (100 mg/mL in dichloromethane). Then, sodium alginate and sodium tripolyphosphate (TPP, 220 mg) were fully dissolved in the resulting GSNO-NP suspension. Over an ice bath, calcium chloride solution ($CaCl_2$, 2 M) was added dropwise into this mixture to cross-link alginate homogenized by sonication (40 W, ultrasonic processor, France). GSNO-loaded alginate/chitosan nanocomposites particles (GSNO-acNCPs) were finally formed by dropwise addition of GSNO-NP-alginate mixture into the chitosan solution (1 mg/mL in 1% (v/v) acetic acid), under mechanical stirring (1300 rpm) over ice bath.

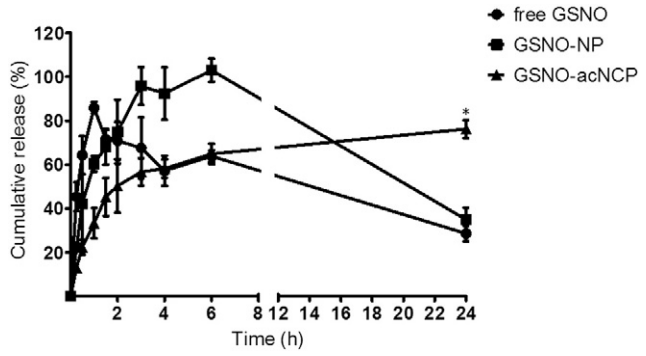

Figure 1. Release kinetic of the payload (GSNO and nitrite ions) from polymer nanocomposite particles in phosphate buffered saline (0.148 M) at 37 °C. Data are shown as mean ± sd, $n = 3$. *: $P < 0.05$ *vs* free GSNO and GSNO-NP (two-way ANOVA). GSNO-NP: GSNO-loaded nanoparticles, GSNO-acNCPs: GSNO-loaded alginate/chitosan nanocomposite particles.

Characterization of GSNO-loaded alginate/chitosan nanocomposite particles

Determination of size. The volume particle size distribution of GSNO-acNCPs was determined by the laser diffraction method (Mastersizer 2000, Malvern Instruments, France). The GSNO-acNCPs were suspended in ultrapure water. The size of GSNO-acNCPs was described by the volume mean diameter measured in triplicate.

Evaluation of GSNO encapsulation efficiency. Encapsulation efficiency (EE) describes the quantity of the drug entrapped within GSNO-acNCPs compared with the initial drug amount. It was determined according to the following equation:

$$EE = m_e/m_i \times 100$$

where EE is the encapsulation efficiency in percent (%), m_e is the mass of drug entrapped in particles, and m_i is the initial mass of drug. The entrapped drug within particles was evaluated by a two-step-liquid–liquid extraction. The external matrix of particles composed of sodium alginate and chitosan was disrupted by mechanical stirring followed by centrifugation and the amount of GSNO remaining in the supernatant, subtracted by the free nitrite ions quantified by the Griess assay,[34] was quantified by the Griess–Saville assay using sulfanilamide and $HgCl_2$ in acidic conditions to cleave the *S*-NO bond, and *N*-(1-napthyl)ethylenediamine to form a chromophoric azo product that absorbs at 540 nm.[34]

The resulting pellet, which corresponds to GSNO-NPs, was dissolved in 2 mL dichloromethane and the amount of GSNO in the nanoparticles was extracted in phosphate buffered saline (PBS) at pH 7.4 and determined by the Griess–Saville assay as described above. All the samples were prepared in triplicate.

Core loading expressed in mg of GSNO/g of polymer was estimated from initial GSNO, Eudragit® RL PO, sodium alginate and chitosan amounts.

In vitro release kinetic. GSNO-acNCPs were suspended in 1 mL of PBS and were placed in cellulose dialysis tubing (average flat width 10 mm (0.4 in), cut-off 14 kDa). Release kinetic was measured as previously described[27] in 200 mL of PBS at 37 °C protected from light. The GSNO and nitrite ions released were monitored every 30 min during two hours, every hour from two to six hours, then at 24 h, and immediately quantified with a fluorometric method[35] using diaminonaphthalene (added or not with $HgCl_2$ to cleave the *S*-NO bond) producing naphthotriazole (emission 415 nm/excitation 375 nm, JASCO FP-8300, France).

Stability of GSNO in GSNO-loaded alginate/chitosan nanocomposite particles. The GSNO-acNCP or GSNO-NP suspensions were centrifuged (15,000 *g*, 20 min, 4 °C) and the resulting pellets were kept in a freezer at −20 °C, in a fridge at +4 °C or at +37 °C in a humidified incubator. At predetermined time intervals over 15 days (D) (1D, 2D, 3D, 4D, 5D and 15D), the GSNO was extracted and analyzed by the Griess–Saville assay as above to determine the remaining intact and decomposed GSNO. All the samples were prepared in triplicate.

Mucins binding assay

Changes in size and zeta potential of GSNO-NPs in contact with a mucin dispersion were examined.[36] After centrifugation (42,000 *g*, 30 min, 4 °C; Heraeus Instruments, France), nanoparticles were resuspended in a mucin dispersion at a concentration of 5 mg/mL polymer in 1 mg/mL mucin (ratio 5:1). The volume particle size distribution of GSNO-NPs was determined by the laser diffraction method (Mastersizer 2000, Malvern Instruments, France) and zeta potential was estimated by electrophoretic mobility (ZetaSizer NanoZS, Malvern Instruments, France).

Cytocompatibility

The cytocompatibility of GSNO-acNCPs was evaluated on intestinal Caco-2 cells ATCC® HTB-37™. Caco-2 cells were grown in complete medium consisting of Eagle's Minimum Essential Medium EMEM supplemented with 20% (v/v) fetal bovine serum, 4 mM of glutamine, 100 U/mL of penicillin, 100 U/mL of streptomycin, 1% (v/v) of non-essential amino acids. Cells were cultivated at 37 °C under 5% CO_2 (v/v) in a humidified incubator. Caco-2 cells were seeded in 96-wells plates at 20,000 cells/well 24 h before experiment. They were then exposed to 0.5, 1.0, 5.0, 10.0 or 50.0 mg/mL of GSNO-acNCP for 24 h at 37 °C, complete medium being used as control. Cytocompatibility expressed by metabolic activity was checked with the 3(4,5-dimethylthiazol-2-yl)-2,5-diphenyltetrazolium bromide (MTT) assay. The absorbance of extracted formazan crystals was read at 570 nm with a reference at 630 nm (EL 800 microplate reader, Bio-TEK Instrument, Inc®, France). Metabolic activity in control condition was considered as 100%.

In vitro cell permeability

The permeability of GSNO across the Caco-2 monolayer was evaluated in the apical-to-basolateral direction in Hank's Balanced Salt Solution (HBSS, pH 6.5). After seeding 10^6 cells on cell culture inserts (Transwell®, Corning, USA) with 0.4 μm pore size disposed in a 12-wells plate, the medium was replaced every two days during the first week and every day during the lasting days until the differentiated cell monolayer was formed (14-18 days, 588 ± 44 Ω/cm^2). For

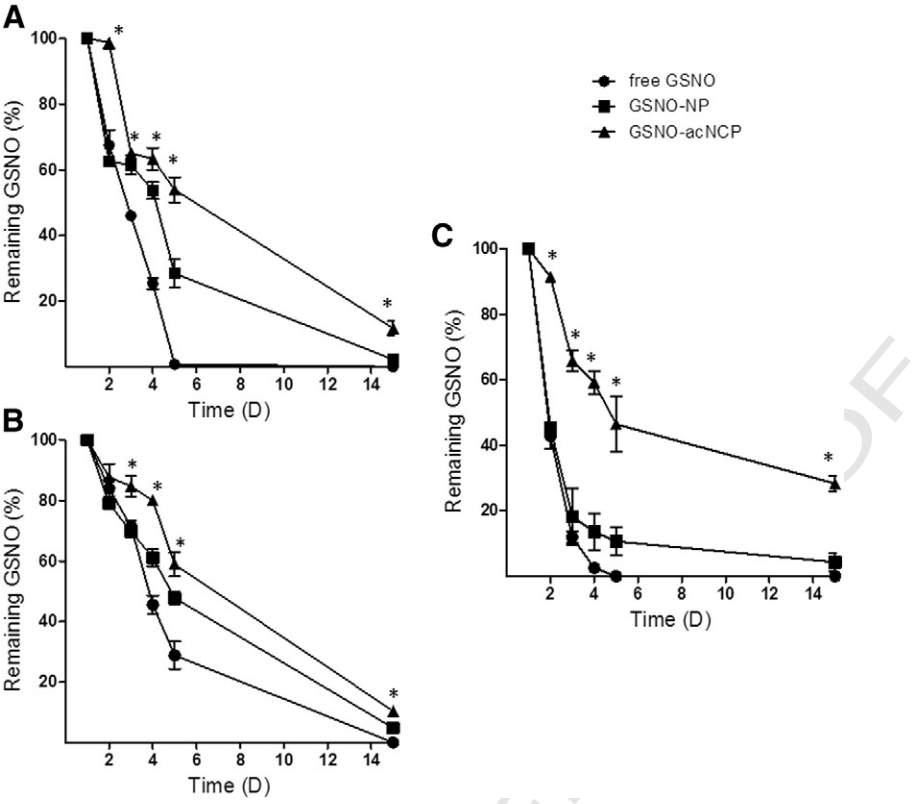

Figure 2. Stability of GSNO in polymer particles. GSNO-loaded alginate/chitosan nanocomposite particles (GSNO-acNCPs) or GSNO-loaded nanoparticles (GSNO-NP) suspensions were centrifuged and the resulting pellets were stored at −20 °C **(A)**, +4 °C **(B)** and +37 °C **(C)** for 15 days. At regular intervals, the remaining intact GSNO was determined by the Griess–Saville assay. Data are expressed as mean ± sd (n = 3). *: $P < 0.05$ *vs* free GSNO (two-way ANOVA).

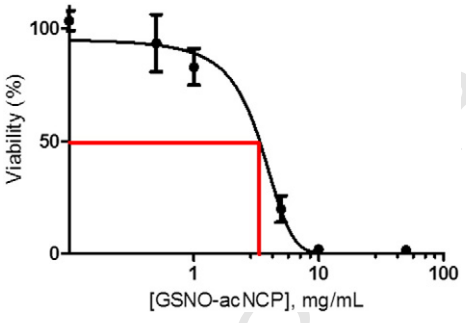

Figure 3. *In vitro* cytotoxicity of polymer nanocomposite particles on Caco-2 cells. Caco-2 cells were treated with the indicated concentrations of GSNO-loaded alginate/chitosan nanocomposite particles (GSNO-acNCPs) for 24 h at 37 °C. Viability was estimated through mitochondrial activity by the MTT assay. Data are expressed as mean ± sem (n = 3).

the permeation experiments, polymer nanocomposite particles containing 50 μM of GSNO were suspended in 500 μL of HBSS and introduced in the apical (donor) compartment, whereas, 1.5 mL of HBSS was placed in basolateral (receptor) compartment. After 1, 4 and 24 h, each basolateral compartment was withdrawn and replaced with the same volume of fresh HBSS. The GSNO, nitrite and nitrate ions permeated and presented in basolateral (for each time) and apical (after 24 h only) compartments were detected using the fluorometric method.[26]

The integrity of the cell monolayer was checked before the permeability studies by measuring the transepithelial electrical resistance (TEER) using a Millicell®-Electrical Resistance system (Millipore, USA). In addition, the permeation of fluorescein sodium (5 μM) was also used to verify the integrity of monolayer.

The cumulative amounts of GSNO crossing the Caco-2 monolayer were calculated from the concentrations measured in basolateral compartments. The apparent permeability coefficient (Papp) values were calculated using the following equation:

$$\text{Papp} = \frac{dQ}{dt} \times \frac{1}{A \times C_0}$$

dQ/dt (mol/s) refers to the permeability rate (mol) of RSNO in the basolateral compartment at the time of quantification, A (cm^2) refers to membrane diffusion area, and C_0 (mol/mL) refers to the initial concentration in the apical compartment.

The enhancement ratio (R) was calculated through the following equation:

$$\text{R} = \text{Papp1}/\text{Papp2}$$

Papp1 refers to the apparent permeability coefficient of each treatment, and Papp2 corresponds to the apparent permeability coefficient of free GSNO.

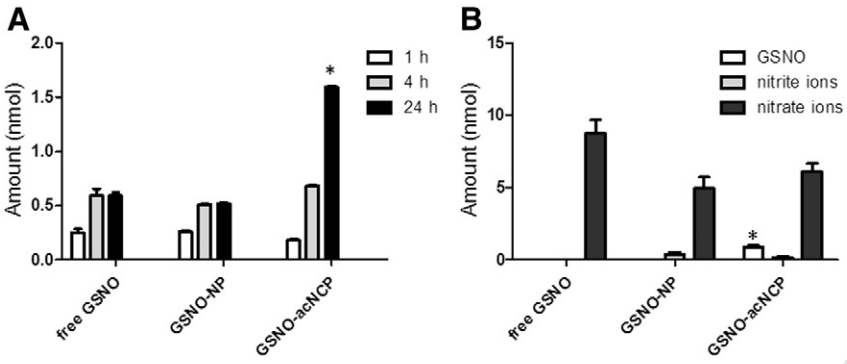

Figure 4. Caco-2 cell permeability of GSNO from polymer particles. Twenty five nmol of free GSNO or equivalent amount of GSNO-loaded nanoparticles (GSNO-NP) or GSNO-loaded alginate/chitosan nanocomposite particles (GSNO-acNCPs) were loaded in the apical compartment of a transwell® system seeded with Caco-2 cells 15 days before. **(A)** Amount of GSNO permeated from the apical to the basolateral compartment after 1 h, 4 h or 24 h. **(B)** Amount of the different nitric oxide species remained in the apical compartment after 24 h. Values presented have been corrected from control (cells without treatment for free GSNO, blank formulations for GSNO loaded formulations). Data are shown as mean ± sem (n = 3). *: $P < 0.05$ *vs* free GSNO and GSNO-NP (two-way ANOVA).

Ex vivo pharmacological evaluation

Animals used and ethical statement. Vasorelaxation was evaluated on endothelium-removed aortic rings isolated from 12 week-old, male, normotensive, Wistar rats (Janvier Laboratories, Le Genest-St-Isle, France; 400-500 g). All experiments were performed in accordance with the European Community guidelines (2010/63/EU) for the use of experimental animals in the respect of the 3 Rs' requirements for Animal Welfare (C. Perrin-Sarrado permit number n°54-72, I. Lartaud n° 54-5; the project untitled "Nitro-Vivo" was positively evaluated the19th of December 2014 by the CELMEA (regional ethical committee for animal experiments) and approved by the French Ministry of Research n°APAFIS1614-2015090216575422v2). Animals were kept under standard conditions (temperature: 21 ± 1 °C, hygrometry 60 ± 10%, light on from 6 am to 6 pm) and had free access to standard diet (A04, Safe, Villemoisson-sur-Orge, France) and water (reverse osmosis system, Culligan, Brussells, Belgium).

Treatment schedule. GSNO-acNCPs (15 mg of GSNO/kg body weight), free GSNO (15 mg of GSNO/kg body weight), blank-acNCPs or PBS as controls were administrated by gavage (10 mL/kg of rat) to Wistar rats (fasted 8 h before gavage). Seventeen hours after gavage, rats were sacrificed by exsanguination after anesthesia (sodium pentobarbitone 60 mg/kg, intraperitoneal, Sanofi Santé Nutrition Animale, Libourne, France) and intravenous administration of heparin (500 U, Heparine Choay). A segment (around 3 cm) of the descending thoracic aorta was removed and immediately placed in cold Krebs' solution. Vessels were cleaned from surrounding connective tissues and cut into 2-mm long rings (8 rings per rat). The endothelium was removed by rubbing the intimal surface of the rings with forceps and immediately used for *ex vivo* vasoactivity studies.

Measurement of vasoactivity. Aortic vasoactivity was measured using an isometric tension recording system in 10 mL organ chambers (EMKABATH, Emka Technology, France). Baths were filled with Krebs' solution (10 mL, 37 °C, pH 7.4) and continuously bubbled with 95% O_2 and 5% CO_2. Following 60-min equilibration with a basal resting tension determined at 2 g, viability of aortic rings was assessed with potassium chloride (KCl, 6×10^{-2} M) added in the baths. The contraction rapidly reached a steady state and was expressed, after 15 min exposure, as the developed tension from the basal resting tension of 2 g. Arteries showing less than 2.5 g of developed tension were excluded. After viability test and a 30 min wash-out period so that tension returns to baseline, aortic rings were tested with two protocols: i) vasoconstriction of aortic rings (n = 10-12 per group, from 4 different rats in each group) was measured with increasing concentrations of phenylephrine (PHE) (10^{-10} M to 3×10^{-5} M); ii) NO storage in the aorta was evaluated with *N*-acetylcysteine (NAC) used to displace NO from cysteine-NO residue. Rings (n = 10-12 per group, from 4 different rats in each group) preconstricted with 10^{-6} M PHE, were added with NAC (10^{-5} M and 10^{-4} M). Contractile effects were expressed as induced developed tension (Delta T, g) and relaxant ones in percentage of contraction (100% being the stable tension caused by 10^{-6} M PHE).

The absence of functional endothelium was confirmed by the ability of carbachol 10^{-5} M, a muscarinic receptors agonist, to induce less than 10 % of relaxation on 10^{-6} M PHE-preconstricted aortic rings.

Statistical analysis

Results are shown as either mean ± standard deviation (sd) or mean ± standard error of the mean (sem) values. The half maximal effective concentration (EC_{50}) and maximal response (E_{max}) were calculated by fitting each concentration response curve using the Hill logistic equation. For the comparison of Papp, and that of E_{max} and EC_{50} for PHE, statistical comparisons were performed using the one-way ANOVA ($P < 0.05$). Other analyses were performed using the two-way ANOVA ($P_{treatment} < 0.05$; $P_{time} < 0.05$). Statistical analyses were performed using the GraphPad Prism software (GraphPad Software version 5.0, San Diego, USA).

t1.1 Table 1
t1.2 Apparent permeability coefficient (Papp) and enhancement ratio (R) of GSNO permeation across Caco-2 monolayers.

t1.3 Group	Papp (10^{-8} cm/s)	R
t1.4 Free GSNO	8.3 ± 0.3	1.0
t1.5 GSNO-NP	7.7 ± 3.1	0.9
t1.6 GSNO-acNCPs	34.1 ± 1.5*	4.1

t1.7 Data are shown as mean ±sem, $n = 3$. All data sets were compared to free GSNO. *: $P < 0.05$ *vs* free GSNO (one-way ANOVA). GSNO-NP: GSNO-loaded nanoparticles, GSNO-acNCPs: GSNO-loaded alginate/chitosan nanocomposite particles.

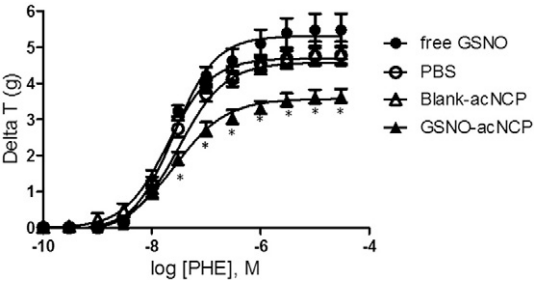

Figure 5. Contractile effect of phenylephrine (PHE) on aortic rings isolated from rats orally treated with free GSNO or GSNO-loaded polymer nanocomposite particles (GSNO-acNCPs) at 15 mg of GSNO/kg of body weight, 17 h before. Blank alginate/chitosan nanocomposite particles (Blank-acNCPs) and phosphate buffered saline (PBS) have been used as controls. Results are expressed as mean ± sem (n = 10-12 per group, from 4 different rats in each group). *: $P < 0.05$ *vs* PBS (two-way ANOVA).

Results

Physico-chemical characterization of GSNO-loaded alginate/chitosan nanocomposite particles

The average size of the developed nanocomposite particles was 56 ± 15 μm (mean ± sd; $n = 3$). GSNO was entrapped within the nanocomposite particles with a high encapsulation efficiency (76 ± 10%), corresponding to an estimated core loading of 15.0 ± 1.9 mg of GSNO/g of polymer. The inner core of GSNO loaded nanoparticles presented an estimated core loading of 5.7 mg of GSNO/g of polymer with a zeta potential of +40 ± 6 mV and a mean diameter of 0.289 ± 0.014 μm.[26] As shown in Figure 1, 75 ± 3% of free GSNO was released from the dialysis bag during the first hour. Similarly, GSNO-NPs showed a release profile with a burst release of 95 ± 2% of the initially loaded GSNO within the first 3 h. On the other hand, only 57 ± 6% of GSNO was released from GSNO-acNCPs within 3 h and the remaining amount was released in a sustained way over the next 21 h.

Stability of GSNO in GSNO-loaded alginate/chitosan nanocomposite particles

The stability of GSNO within the polymer nanocomposite particles was evaluated at −20 °C, +4 °C and +37 °C. After 5 days of storage at −20 °C or +4 °C, 100 ± 1% or 70 ± 5% of free GSNO respectively, was decomposed (Figure 2, *A*, *B*). When incorporated into the polymer nanocomposite particles, 16 ± 5% (−20 °C) and 12 ± 4% (+4 °C) of intact GSNO was preserved for 15 days, showing improvement of GSNO stability. At +37 °C, GSNO degraded faster (Figure 2, *C*): 57 ± 4% of free GSNO had decomposed within two days and 98 ± 1% after 4 days. Polymer nanocomposite particles increased the life-time of GSNO as 46 ± 9% and 12 ± 4% of intact GSNO were detected on the 4th and 15th days respectively.

Mucin binding assay

The mucoadhesion property of the polymeric GSNO-NPs was also evaluated. The diameter of GSNO-NPs in contact with mucin dispersion immediately increased from 0.2 ± 0.0 μm to 18.2 ± 3.2 μm (100 times more) and estimated zeta potential value was divided per 3 (from +54 ± 4 mV to +18 ± 5 mV, (mean ± sd; $n = 3$)).

Cytocompatibility and cell permeability

The concentration-response curve built from the MTT metabolic activity assay (Figure 3) gave an IC_{50} at 3.24 ± 0.38 mg/mL for GSNO-acNCPs. Therefore, a concentration of 1 mg/mL (containing 50 μM GSNO) that maintained 83 ± 1% of cell viability was chosen for Caco-2 permeability studies.

Caco-2 cell monolayers were incubated with 50 μM (representing 25 nmol of GSNO in 0.5 mL) free or nanoparticle-associated GSNO in the apical compartment to investigate GSNO permeability. After 1 h of incubation, a similar concentration of GSNO was detected in the basolateral compartment for all formulations (Figure 4, *A*). The permeation kinetics of the RSNO were similar for GSNO and GSNO-NPs: the amount transported rose rapidly to 0.59 ± 0.07 nmol and 0.51 ± 0.01 nmol, respectively, over the first 4 h, and then remained at a plateau up to 24 h. GSNO-acNCPs showed a steady penetration rate over the whole 24 h, and promoted 2.7-fold more GSNO crossing the cell monolayer than free GSNO or GSNO-NP (Figure 4, *A*). The Papp value of GSNO (showing the ability of NPs and acNCPs to help the transport of GSNO across Caco-2 cell monolayer) did not change with NP, but significantly increased after GSNO-NPs incorporation into nanocomposite particles, showing an enhancement ratio of 4.1 (Table 1). In contrast to free GSNO and GSNO-NPs, GSNO-acNCPs retained 0.9 ± 0.1 nmol of intact GSNO in the apical compartment after 24 h of incubation (Figure 4, *B*) showing that GSNO-acNCPs could have an even longer release profile.

At the end of experiments, the test using the low molecular weight hydrophilic tracer sodium fluorescein, showed that the permeation of sodium fluorescein in the treated groups (18 ± 5%) was higher than the positive control (6.1 ± 0.5%) and less than negative control (32 ± 9%), in which cells were treated with HBSS without Ca^{2+} and Mg^{2+}. Taken together, these results confirmed the integrity of cells monolayer after incubation with the GSNO-acNCPs with a slight opening of tight junction due to chitosan.

GSNO-NPs[26] showed a core loading two times under the GSNO-acNCPs core loading (5.7 mg of GSNO/g of polymer

t2.1 Table 2
Half maximum effective concentration (EC_{50}) and maximum effect (E_{max}) of
t2.2 phenylephrine measured in isolated aortic rings.

t2.3 Group	EC_{50} (10^{-8} M)	E_{max} (g)
t2.4 PBS	3.1 ± 0.1	4.8 ± 0.1
t2.5 Blank-acNCPs	1.9 ± 0.2	4.8 ± 0.3
t2.6 Free GSNO	3.1 ± 0.1	4.9 ± 0.1
t2.7 GSNO-acNCPs	3.1 ± 0.1	3.7 ± 0.1*

Data are shown as mean ±sem, (n = 10-12 per group, from 4 different rats in each group). *: $P < 0.05$ *vs* PBS (one-way ANOVA). PBS: phosphate buffered saline. Blank-acNCPs: blank alginate/chitosan nanocomposite particles,
t2.8 GSNO-acNCPs: GSNO-loaded alginate/chitosan nanocomposite particles.

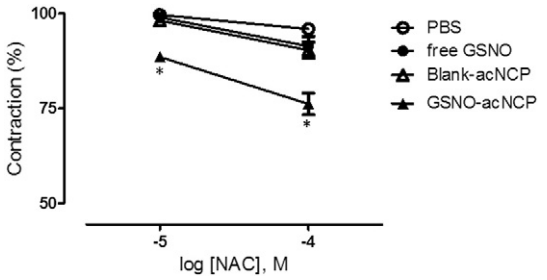

Figure 6. Vascular effect of 10^{-5} M and 10^{-4} M *N*-acetylcysteine (NAC) on precontracted (10^{-6} M phenylephrine) aortic rings isolated from rats orally treated with free GSNO or GSNO-loaded polymer nanocomposite particles (GSNO-acNCPs) at 15 mg of GSNO/kg of body weight, 17 h before. Blank alginate/chitosan nanocomposite particles (Blank-acNCPs) and phosphate buffered saline (PBS) have been used as controls. Results are expressed as mean ± sem (n = 10-12 per group, from 4 different rats in each group). *: $P < 0.05$ *vs* PBS (two-way ANOVA).

and 15.0 ± 1.9 mg of GSNO/g of polymer, respectively). Furthermore, the permeability studies failed in showing a higher and long lasting absorption of GSNO for the GSNO-NPs through intestinal cells compared to free GSNO. For these two reasons, the GSNO-NPs were moved aside from the *in vivo* studies

Pharmacological vascular effects

The dose–response curves to PHE were similar in aortic rings from Wistar rats orally treated 17 h earlier with free GSNO, blank-acNCP or PBS (Figure 5). In aortic rings from rats treated with GSNO-acNCP (15 mg/kg body weight), the contractile maximal effect (E_{max}) of PHE significantly decreased (from 4.8 g in control groups to 3.7 g in the GSNO-acNCP group, −25%, $P < 0.05$) with no change in EC_{50} (Table 2).

In all the control groups, NAC failed to relax the vessels. However, in the group treated with GSNO-acNCP, NAC induced significant relaxation (11 ± 1% at 10^{-5} M and 24 ± 3% at 10^{-4} M, $P < 0.05$ compared to controls, Figure 6).

Discussion

The encapsulation of the fragile molecule GSNO within drug delivery systems is still challenging. Different approaches, either through *S*-nitrosation of free or conjugated GSH[23,25] or direct encapsulation of GSNO[21,37] are described in the literature. In the present study, we adopted the second approach with gentle formulation process to develop polymer nanocomposite particles loaded with GSNO. The polymer nanocomposites were obtained by incorporation of GSNO loaded Eudragit® RL nanoparticles (GSNO-NP)[26] into a polymer matrix prepared from a mixture of alginate and chitosan by ionic gelation. The challenge was to control the loading of GSNO within the nanocomposite particles in order to get potential pharmacological efficiency. We based our calculations on the minimal concentration of NO required to stimulate the synthesis of cyclic GMP by soluble guanylate cyclase in vascular smooth muscle (approximately 10 nmol/L[38]), and the dose of GSNO that significantly decreases mean arterial blood pressure (*i.e.* 3 mg; 100 μg/min for 30 min, intravenous, in human[39]).

Compared to our previous published results on GSNO-NP,[26] the newly formulated composite particles improved the loading capacity of GSNO by 2.6-fold (from 5.7 to 15.0 mg of GSNO/g of polymer). This improvement can probably be attributed to the use of alginate and chitosan, which are hydrophilic and have good affinity for GSNO thus allowing the entrapment not only of GSNO-NP but also of the free GSNO remaining outside the nanoparticles. This is consistent with our previously reported polymer nanocomposites based on chitosan or alginate separately.[27]

Our results on *in vitro* release demonstrate that the polymer nanocomposite particles prevented the burst release of hydrophilic GSNO observed with GSNO-NP alone. This is in agreement with the results of Hasan et al[40] showing that composite particles were able to reduce the burst release. GSNO-acNCPs present two polymer barriers to the diffusion of GSNO: the first being formed by the hydrophobic Eudragit® RL polymer and the second by the outer hydrophilic matrix composed of chitosan and alginate. The combination of both leads the diffusion distance to increase and the release rate to slow down. Furthermore, as reported by de Seabra et al[20,41,42] increased microviscosity of the solvent improve the stability of RSNO. The presence of alginate and chitosan, which build a hydrophilic matrix for the particles, increases the viscosity thereby protecting GSNO from thermal decomposition and improved GSNO stability. Moreover, the increased stability we obtained at +37 °C for GSNO-acNCPs was in accordance with our previous observations using alginate or chitosan in polymer nanocomposite particles.[27]

GSNO-acNCPs also improved the permeability of GSNO through the Caco-2 cells model, and increased the Papp value, a marker of drug absorption. This permeation enhancement may be attributed to three major factors: i) the positive charge of GSNO-acNCPs (zeta potential approximately equal to +18.5 ± 0.8 mV), which allows electrostatic attraction with the negatively charged cell membrane; ii) the composition of nanocomposite particles based on chitosan and alginate, which have mucoadhesive properties and reinforce the interaction with cells; iii) the high level of protection of GSNO afforded by the nanocomposite particles. While we did not directly measure GSNO crossing through intestinal tissue, our results augur a promising oral delivery, for which intestinal absorption is one of the key factors determining drug bioavailability. The mechanisms involved in intestinal crossing remain to be evaluated. However, the glycosidic bonds of chitosan were shown to be rapidly hydrolyzed under gastric conditions,[43] so only a portion

of this polymer and the alginate of the complex matrix will be able to adhere on the mucus layer and to open tight junctions in the intestinal compartment.[44] Moreover, alginate will help the inner core made of GSNO-NPs to penetrate the mucus layer. GSNO-NPs will no longer stay at the nanometer size: as we showed they adsorb proteins like mucins or albumin[26] to reach a final size around 20 μm. Others also showed that the mucus layer strongly increase particle size and modify absorption of particles through the intestine.[45] Indeed, Bajka et al demonstrated that a particle diameter higher than 500 nm largely decreased particles diffusion.[45] Therefore, it is probable that only GSNO or other NO species will diffuse within the intestinal tight junctions, already opened by chitosan, and reach the vascular compartment.

Whatever the mechanisms involved in intestinal crossing, oral administration of GSNO-acNCPs to Wistar rats reveals NO-related vascular effects attesting that NO effectively reaches the blood stream. The decreased contractile response of aorta to PHE is the proof that the absorbed GSNO is transported from the intestine to the aortic wall by itself or through transnitrosation process of albumin or hemoglobin in the blood stream. Then, close to the vascular wall, transnitrosation processes occur again to generate a NO store inside the vascular wall. The final storage of NO in vascular smooth muscle cells was highlighted by aortic hyporeactivity to PHE and vasorelaxation in response to NAC. Indeed, in the absence of NO storage, NAC is not able to relax aortic rings, whereas, in presence of NO stores (*S*-nitrosation of proteins/peptides cysteine residues) within the vessel wall, NAC after entering into the cells displaces NO from vascular stores, which finally activates the guanylate cyclase/GMPc pathway inducing relaxation. Finally, the transnitrosation reactions with *S*-nitrosated proteins/peptides,[46] leading to the formation of unstable *S*-nitrosothiols may be involved, both in the storage processes during the 17 hours following gavage, and in the release of NO induced by NAC.[47] Similar results were obtained *ex vivo* in previous experiments where NO donors applied directly on the aortic rings, sustained hyporeactivity to vasoconstrictors from 1 to 4 hours.[47-50] Oral administrations of PBS or blank-acNCPs, as that of free GSNO – due to its limited stability – were unable to form a reservoir of NO in vascular tissue, and NAC has no vasorelaxant effect.

Another hypothesis for the decreased response to PHE may relate to the *S*-nitrosation of the alpha1–adrenergic receptor leading to its decreased affinity for sympathetic ligands.[51] This is unlikely in the present study as EC_{50} remained similar in all groups of treatment.

In conclusion, we demonstrated the therapeutic potential of polymer nanocomposite particles based on poly(methyl)methacrylate inside an alginate plus chitosan matrix for oral delivery of GSNO. The efficient loading, protection and sustained release of GSNO provided by these formulations promote GSNO absorption through the intestinal barrier, allow GSNO to reach the blood stream and contribute to form a reservoir of NO by transnitrosation inside the vascular wall. Seventeen hours following oral administration, vascular hyporeactivity to the vasoconstrictor remained. These new drug delivery systems of NO donors may be particularly adapted for oral treatment of cardiovascular diseases.

Acknowledgments Q4

The authors are grateful to Dr. François Dupuis, Patrick Liminana and Isabelle Fries (EA 3452, CITHEFOR, Lorraine University) for the helpful advices and technical support to experimental studies, Pr Gillian Barratt (UMR CNRS 861, Paris-Sud University) for manuscript spelling corrections.

References Q3

1. Versari D, Daghini E, Virdis A, Ghiadoni L, Taddei S. Endothelium-dependent contractions and endothelial dysfunction in human hypertension. *Pharmacol* 2009;**157**:527-36, http://dx.doi.org/10.1111/j.1476-5381.2009.00240.x.
2. Davignon J, Ganz P. Role of endothelial dysfunction in atherosclerosis. *Circulation* 2004;**109**:27-32, http://dx.doi.org/10.1161/01.CIR.0000131515.03336.f8.
3. Moncada S, Palmer RM, Higgs EA. Nitric oxide: Physiology, pathophysiology, and pharmacology. *Pharmacol Rev* 1991;**43**:109-42 [doi:0031-6997/91/4302-0109$03.00/0].
4. Cai H, Harrison DG. Endothelial dysfunction in cardiovascular diseases: The role of oxidant stress. *Circ Res* 2000;**87**:840-4, http://dx.doi.org/10.1161/01.RES.87.10.840.
5. Napoli C, de Nigris F, Williams-Ignarro S, Pignalosa O, Sica V, Ignarro LJ. Nitric oxide and atherosclerosis: An update. *Nitric Oxide* 2006;**15**:265-79.
6. Sim Ji-Yeon. Nitric oxide and pulmonary hypertension. *Anesthesiol* 2010;**58**:4-14, http://dx.doi.org/10.4097/kjae.2010.58.1.4.
7. Loscalzo J. Nitric oxide insufficiency, platelet activation, and arterial thrombosis. *Circ Res* 2001;**88**:756-62, http://dx.doi.org/10.1161/hh0801.089861.
8. Bolaños JP, Almeida A. Roles of nitric oxide in brain hypoxia-ischemia. *Biochim Biophys Acta* 1999;**1411**:415-36, http://dx.doi.org/10.1016/S0005-2728(99)00030-4.
9. Tamargo J, Caballero R, Gómez R, Delpón E. Cardiac electrophysiological effects of nitric oxide. *Cardiovasc Res* 2010;**87**:593-600, http://dx.doi.org/10.1093/cvr/cvq214.
10. Hogg N, Singh RJ, Kalyanaraman B. The role of glutathione in the transport and catabolism of nitric oxide. *FEBS Lett* 1996;**382**:223-8, http://dx.doi.org/10.1016/0014-5793(96)00086-5.
11. Riccio DA, Dobmeier KP, Hetrick EM, Privett BJ, Paul HS, Schoenfisch MH. Nitric oxide-releasing *S*-nitrosothiol-modified xerogels. *Biomaterials* 2009;**30**:4494-502, http://dx.doi.org/10.1016/j.biomaterials.2009.05.006.
12. Langford EJ, Brown AS, Wainwright RJ, de Belder AJ, Thomas MR, Smith RE, et al. Inhibition of platelet activity by *S*-nitrosoglutathione during coronary angioplasty. *Lancet* 1994;**344**:1458-60, http://dx.doi.org/10.1016/S0140-6736(94)90287-9.
13. MacAllister RJ, Calver AL, Riezebos J, Collier J, Vallance P. Relative potency and arteriovenous selectivity of nitrovasodilators on human blood vessels: An insight into the targeting of nitric oxide delivery. *J Pharmacol Exp Ther* 1995;**273**:154-60.
14. Rassaf T, Kleinbongard P, Preik M, Dejam A, Gharini P, Lauer T, et al. Plasma nitrosothiols contribute to the systemic vasodilator effects of intravenously applied NO: Experimental and clinical study on the fate of NO in human blood. *Circ Res* 2002;**91**:470-7, http://dx.doi.org/10.1161/01.RES.0000035038.41739.CB.
15. Friedman AJ, Blecher K, Schairer D, Tuckman-Vernon C, Nacharaju P, Sanchez D, et al. Improved antimicrobial efficacy with nitric oxide releasing nanoparticle generated *S*-nitrosoglutathione. *Nitric Oxide* 2011;**25**:381-6, http://dx.doi.org/10.1016/j.niox.2011.09.001.
16. Sorragi Cde L, Shishido SM, Lemos ME, Marcondes S, Antunes E, Krieger MH. *In vitro* evaluation of the safe margin, antithrombotic and antiproliferative actions for the treatment of restenosis: Nitric oxide

donor and polymers. *Cell Biochem Funct* 2011;**29**:207-14, http://dx.doi.org/10.1002/cbf.1738.

17. Jensen DE, Belka GK, Du Bois GC. *S*-Nitrosoglutathione is a substrate for rat alcohol dehydrogenase class III isoenzyme. *Biochem J* 1998;**331**(Pt 2):659-68.
18. Bateman RL, Rauh D, Tavshanjian B, Shokat KM. Human carbonyl reductase 1 is an *S*-nitrosoglutathione reductase. *J Biol Chem* 2008;**283**:35756-62, http://dx.doi.org/10.1074/jbc.M807125200.
19. Chen Q, Sievers RE, Varga M, Kharait S, Haddad DJ, Patton AK, et al. Pharmacological inhibition of *S*-nitrosoglutathione reductase improves endothelial vasodilatory function in rats *in vivo*. *J Appl Physiol* 2013;**114**:752-60, http://dx.doi.org/10.1152/japplphysiol.01302.2012.
20. Seabra AB, de Souza GF, da Rocha LL, Eberlin MN, de Oliveira MG. *S*-Nitrosoglutathione incorporated in poly(ethylene glycol) matrix: Potential use for topical nitric oxide delivery. *Nitric Oxide* 2004;**11**:263-72, http://dx.doi.org/10.1016/j.niox.2004.09.005.
21. Seabra AB, da Rocha LL, Eberlin MN, de Oliveira MG. Solid films of blended poly(vinyl alcohol)/poly(vinyl pyrrolidone) for topical *S*-nitrosoglutathione and nitric oxide release. *J Pharm Sci* 2005;**94**:994-1003, http://dx.doi.org/10.1002/jps.20314.
22. de Mel A, Naghavi N, Cousins BG, Clatworthy I, Hamilton G, Darbyshire A, et al. Nitric oxide-eluting nanocomposite for cardiovascular implants. *J Mater Sci Mater Med* 2014;**25**:917-29, http://dx.doi.org/10.1007/s10856-013-5103-2.
23. Marcato PD, Adami LF, de Melo Barbosa R, Melo PS, Ferreira IR, de Paula L, et al. Development of a sustained-release system for nitric oxide delivery using alginate/chitosan nanoparticles. *Curr Nanosci* 2013;**9**:1-7, http://dx.doi.org/10.2174/157341313805117848.
24. Marcato PD, Adami LF, Melo PS, de Paula L, Durán N, Seabra AB. Glutathione and *S*-nitrosoglutathione in alginate/chitosan nanoparticles: Cytotoxicity. *JPCS* 2011;**304**:012045, http://dx.doi.org/10.1088/1742-6596/304/1/012045.
25. Shah SU, Martinho N, Socha M, Pinto Reis C, Gibaud S. Synthesis and characterization of *S*-nitrosoglutathione-oligosaccharide-chitosan as a nitric oxide donor. *Expert Opin Drug Deliv* 2015;**12**:1-15, http://dx.doi.org/10.1517/17425247.2015.1028916.
26. Wu W, Gaucher C, Diab R, Fries I, Xiao YL, Hu XM, et al. Time lasting *S*-nitrosoglutathione polymeric nanoparticles delay cellular protein *S*-nitrosation. *Pharm Biopharm* 2015;**89**:1-8, http://dx.doi.org/10.1016/j.ejpb.2014.11.005.
27. Wu W, Gaucher C, Fries I, Hu XM, Maincent P, Sapin-Minet A. Polymer nanocomposite particles of *S*-nitrosoglutathione: A suitable formulation for protection and sustained oral delivery. *Pharm* 2015;**495**:354-61, http://dx.doi.org/10.1016/j.ijpharm.2015.08.074.
28. Bhattacharya SN, Kamal MR, Gupta RK. *Polymeric Nanocomposites: Theory and Practice*. Carl Hanser Verlag GmbH & Co. KG978-3-446-40270-6; 20071-13.
29. Gomez-Orellana I. Strategies to improve oral drug bioavailability. *Expert Opin Drug Deliv* 2005;**2**:419-33, http://dx.doi.org/10.1517/17425247.2.3.419.
30. Zhang H, Zhang J, Streisand JB. Oral mucosal drug delivery: Clinical pharmacokinetics and therapeutic applications. *Clin Pharmacokinet* 2002;**41**:661-80, http://dx.doi.org/10.2165/00003088-200241090-00003.
31. Dodane V, Amin Khan M, Merwin JR. Effect of chitosan on epithelial permeability and structure. *Pharm* 1999;**182**:21-32.
32. Thanou M, Verhoef JC, Junginger HE. Oral drug absorption enhancement by chitosan and its derivatives. *Adv Drug Deliv Rev* 2001;**52**:117-26, http://dx.doi.org/10.1016/S0169-409X(01)00231-9.
33. Parent M, Dahboul F, Schneider R, Clarot I, Maincent P, Lerroy P, et al. A complete physicochemical identity card of *S*-nitrosoglutathione. *Curr Pharm Anal* 2013;**9**:31-42.
34. Sun J, Zhang X, Broderick M, Fein H. Measurement of nitric oxide production in biological systems by using griess reaction assay. *Sensors* 2003;**3**:276-84, http://dx.doi.org/10.3390/s30800276.
35. Liu CY, Zhao M, Ren CY, YANG GP, Li PF, Han Y. Direct measurement of nitric oxide in seawater medium by fluorometric method. *Anal Chem* 2009;**37**:1463-7, http://dx.doi.org/10.1016/S1872-2040(08)60136-X.
36. Lim JH, You SK, Baek JS, Hwang CJ, Na YG, Shin SC, et al. Preparation and evaluation of polymeric microparticulates for improving cellular uptake of gemcitabine. *Nanomedicine* 2012;**7**:2307-14, http://dx.doi.org/10.2147/IJN.S30465.
37. Parent M, Boudier A, Fries I, Gostyńska A, Rychter M, Lulek J. Nitric oxide-eluting scaffolds and their interaction with smooth muscle cells *in vitro*. *J Biomed Mater Res A* 2015;**103**:3303-11, http://dx.doi.org/10.1002/jbm.a.35464.
38. Hutchinson PJ, Palmer RM, Moncada S. Comparative pharmacology of EDRF and nitric oxide on vascular strips. *Pharmacol* 1987;**141**:445-51, http://dx.doi.org/10.1016/0014-2999(87)90563-2.
39. Everett TR, Wilkinson IB, Mahendru AA, McEniery CM, Garner SF, Goodall AH, et al. *S*-Nitrosoglutathione improves haemodynamics in early-onset pre-eclampsia. *Clin Pharmacol* 2014;**78**:660-9, http://dx.doi.org/10.1111/bcp.12379.
40. Hasan AS, Socha M, Lamprecht A, Ghazouani FE, Sapin A, Hoffman M, et al. Effect of the microencapsulation of nanoparticles on the reduction of burst release. *Pharm* 2007;**344**:53-61, http://dx.doi.org/10.1016/j.ijpharm.2007.05.066.
41. Seabra AB, De Oliveira MG. Poly(vinyl alcohol) and poly(vinyl pyrrolidone) blended films for local nitric oxide release. *Biomaterials* 2004;**25**:3773-82, http://dx.doi.org/10.1016/j.biomaterials.2003.10.035.
42. Seabra AB, Fitzpatrick A, Paul J, De Oliveira MG, Weller R. Topically applied *S*-nitrosothiol-containing hydrogels as experimental and pharmacological nitric oxide donors in human skin. *Dermatol* 2004;**151**:977-83, http://dx.doi.org/10.1111/j.1365-2133.2004.06213.x.
43. George M, Abraham TE. Polyionic hydrocolloids for the intestinal delivery of protein drugs: Alginate and chitosan – a review. *J Control Release* 2006;**114**:1-14, http://dx.doi.org/10.1016/j.jconrel.2006.04.017.
44. Garrait G, Beyssac E, Subirade M. Development of a novel drug delivery system: Chitosan nanoparticles entrapped in alginate microparticles. *J Microencapsul* 2014;**31**:363-72, http://dx.doi.org/10.3109/02652048.2013.858792.
45. Bajka BH, Rigby NM, Cross KL, Macierzanka A, Mackie AR. The influence of small intestinal mucus structure on particle transport *ex vivo*. *Colloids Surf B: Biointerfaces* 2015;**135**:73-80, http://dx.doi.org/10.1016/j.colsurfb.2015.07.038.
46. Gaucher C, Boudier A, Dahboul F, Parent M, Leroy P. *S*-nitrosation/denitrosation in cardiovascular pathologies: Facts and concepts for the rational design of *S*-nitrosothiols. *Curr Pharm Des* 2013;**19**:458-72.
47. Alencar JL, Lobysheva I, Geffard M, Sarr M, Schott C, Schini-Kerth VB, et al. Role of *S*-nitrosation of cysteine residues in long-lasting inhibitory effect of nitric oxide on arterial tone. *Mol Pharmacol* 2003;**63**:1148-58.
48. Khan SI, Abourashed EA, Khan IA, Walker LA. Transport of harman alkaloids across Caco-2 cell monolayers. *Chem Pharm Bull* 2004;**52**:394-7, http://dx.doi.org/10.1248/cpb.52.394.
49. Megson IL, Greig IR, Gray GA, Webb DJ, Butler AR. Prolonged effect of a novel S-nitrosated glyco-amino acid in endothelium-denuded rat femoral arteries: Potential as a slow release nitric oxide donor drug. *Pharmacol* 1997;**122**:1617-24, http://dx.doi.org/10.1038/sj.bjp.0701557.
50. Megson IL, Morton S, Greig IR, Mazzei FA, Field RA, Butler AR. N-Substituted analogues of S-nitroso-N-acetyl-D, L-penicillamine: Chemical stability and prolonged nitric oxide mediated vasodilatation in isolated rat femoral arteries. *Pharmacol* 1999;**126**:639-48, http://dx.doi.org/10.1038/sj.bjp.0702346.
51. Nozik-Grayck E, Whalen EJ, Stamler JS, McMahon TJ, Chitano P, Piantadosi CA. S-nitrosoglutathione inhibits alpha1-adrenergic receptor-mediated vasoconstriction and ligand binding in pulmonary artery. *Physiol Lung Cell Mol Physiol* 2006;**290**:L136-43, http://dx.doi.org/10.1152/ajplung.00230.2005.

ELSEVIER

Nanomedicine: Nanotechnology, Biology, and Medicine
xx (2016) xxx – xxx

nanomedicine
Nanotechnology, Biology, and Medicine

nanomedjournal.com

Graphical Abstract

Nanomedicine: Nanotechnology, Biology, and Medicine xxx (2016) xxx – xxx

Polymer nanocomposites enhance *S*-nitrosoglutathione intestinal absorption and promote the formation of releasable nitric oxide stores in rat aorta

Wen Wu, PharmD, PhD[a], Caroline Perrin-Sarrado, PharmD, PhD[a], Hui Ming, PharmD[a], Isabelle Lartaud, PharmD, PhD[a], Philippe Maincent, PharmD, PhD[a], Xian-Ming Hu, PhD[b], Anne Sapin-Minet, PhD[a], Caroline Gaucher, PhD[a,*]

[a]*CITHEFOR EA3452 "Drug targets, formulation and preclinical assessment", Faculté de Pharmacie, Université de Lorraine, Nancy, France*
[b]*State Key Laboratory of Virology, Ministry of Education Key Laboratory of Combinatorial Biosynthesis and Drug Discovery, Wuhan University School of Pharmaceutical Sciences, Wuhan, China*

Novel alginate/chitosan nanocomposite particles were successfully developed for the delivery of *S*-nitrosoglutathione (GSNO), a physiological nitric oxide (NO) donor, with improved encapsulation efficiency, sustained-release. The developed nanocomposite particles enhanced intestinal absorption of GSNO and thus promoted the formation of NO stores in the blood vessels after oral administration to Wistar rats.